A Comparative Study of Two Different Numerical Schemes for the Simulation of Nonlinear Dynamics of Heated Falling Thin Films

Mohammad A. Hamza, Ahmad T. Jameel, Waqar Asrar

Abstract*— In this research, an attempt is made to characterise qualitatively the stability and dynamics of an inclined thin liquid film under the influence of instabilities due to thermo-capillarity and evaporative effects as well as van der Waals intermolecular forces, by employing the implicit finite difference method. The results are compared with solutions obtained by the Fourier spectral method. Flow in thin films of a Newtonian liquid on an inclined plane with an adjacent passive gas layer, is well represented by the Navier-Stokes equations, equation of continuity and associated boundary conditions. Long-wave (lubrication) approximation is applied to simplify the governing equations to arrive at a nonlinear partial differential equation, called equation of evolution (EOE). The spatio-temporal evolution of the interfacial instability in the film caused by internal and/or external effects are studied by numerically solving the EOE using the implicit finite difference method. The results of the numerical simulations of our thin film model are compared with those of a similar problem solved using Fourier spectral method from the literature. Simulations show remarkable agreement in the film dynamics predicted by these two methods. The film rupture times obtained using our implicit finite difference scheme closely match with the values obtained from the Fourier spectral method within less than 1% error. This implies that the implicit finite difference method can be satisfactorily employed for the efficient numerical simulation of the thin film flows, and to decipher its nonlinear dynamics reliably.

Keywords: Implicit finite difference; Long-wave instability; Nonlinear dynamics; Spectral method; Thin liquid film.

1. INTRODUCTION

Thin liquid films find wide applications in science and engineering. A liquid film may be considered thin if its thickness is much smaller than its lateral dimensions. In engineering, thin films occur in heat and mass transfer processes and serve to limit fluxes and to protect surfaces, and finds applications in adhesives, paints, tear films and biological membranes. Thin liquid films display a variety of interesting dynamic characteristics. Because the interface between the thin film layer and the atmosphere is deformable, thin films can also develop wave motion. The interfacial waves in a thin film flowing down an inclined plane display fascinating nonlinear phenomena such as complex disordered patterns, solitary waves and transverse secondary instabilities. The film can rupture, leading to holes in the liquid that expose the solid surface to the atmosphere. Thin film flows are governed to a good approximation by the equations of motion simplified by the long wave (lubrication) approximation.

The stability and nonlinear dynamics of flow of thin liquid films on solid planes has been studied extensively over the past decades. Especially, thin liquid films subjected to various physical-chemical effects such as instabilities due to evaporation at the surface, thermocapillarity, and solutal Marangoni effects owing to thermal gradient in the film had been focus of some of the past and recent works. Furthermore, for an inclined film, the effect of gravitational force becomes significant enough to influence the nonlinear dynamics of the film coupled with other forces. There are numerous applications of inclined thin films in industries, such as thin film heat exchangers, falling film gas-liquid contact devices, sodium cooled fast reactors and many more. Especially, heat transfer in inclined thin liquid film flow is of importance in various chemical and biochemical processes such as solid coating, food processing and in systems with evaporative cooling/condensation as well as high throughput heat exchange devices. The understanding of stability, dynamics and morphology of supported thin (<100nm) liquid films are important in phenomena like flotation, adhesion of fluid particles to surfaces, kinetics and thermodynamics of precursor films in wetting heterogeneous nucleation, film boiling/condensation, multilayer adsorption/film pressure, instability of biological films/membranes, and many other areas [1-6].

Revised Manuscript Received on March 10, 2019.

Mohammad A. Hamza, Mechanical Engineering Department, Kulliyyah (Faculty) of Engineering, International Islamic University Malaysia, P.O. Box 10 , Gombak, 50728 Kuala Lumpur. Malaysia

Ahmad T. Jameel, Biotechnology Engineering Department, Kulliyyah (Faculty) of Engineering, International Islamic University Malaysia, P.O. Box 10 , Gombak, 50728 Kuala Lumpur. Malaysia (email: atjameel@iium.edu.my)

Waqar Asrar, Mechanical Engineering Department, Kulliyyah (Faculty) of Engineering, International Islamic University Malaysia, P.O. Box 10 , Gombak, 50728 Kuala Lumpur. Malaysia

Published By:
Blue Eyes Intelligence Engineering
& Sciences Publication

In what follows, we present the results of our numerical simulations of flow in thin liquid films under the influence of intermolecular van der Waals force, thermo-capillary effect and evaporative instabilities at the free surface. Flow in thin Newtonian liquid film on a solid plane and confined by an adjacent passive gas layer is represented by equation of motion, equation of continuity and associated boundary conditions. The external effects due to gravity and van der Waals attraction are generally incorporated in the body force term of the Navier-Stokes equation. These governing equations rewritten using new variables as defined in Hamza [11], are first rescaled using lubrication theory and then simplified using the long-wave analysis of Benny [7] to arrive at a nonlinear partial differential equation, henceforth called the equation of evolution (EOE) [3, 7-11]. The time evolution of the interfacial instability of the film caused by internal and/or external effects was obtained by numerically solving the EOE [10, 11].

To delineate the detailed nonlinear dynamics and surface morphology of thin-film subjected to different type of instabilities, one requires a robust and efficient numerical scheme for the solution of the equation of evolution (EOE). An implicit time-averaged finite difference formulation of the EOE using Crank Nicholson scheme has been used for the numerical solution of our thin-film model. It is interesting to note that the simulation results obtained using our implicit finite difference code greatly conform with the Fourier spectral simulations of Joo et al. [8], as shown in the results section. This clearly proves the efficacy of the implicit finite difference scheme as a reliable alternative to the Fourier spectral method. The results of the finite difference code used in the present work, was validated with respect to the published results of Joo et al. [8] that employed Fourier spectral method. Thereafter, numerical simulations were carried out using our computer code to study the time evolution of surface instabilities in a non-isothermal thin-film by incorporating the gravity and van der Waals forces, besides thermo-capillary and evaporative effects on the surface [10, 11].

2. METHODS

The brief description of the physics of the problem and its mathematical formulation are given in the following paragraphs.

2.1 The thin film model

Consider a thin viscous Newtonian liquid film resting on a uniformly heated rigid plate inclined at angle θ to the horizontal and bounded above by its vapour as shown in Fig. 1. Film is thick enough that a continuum theory of the liquid is applicable. The film is laterally unbounded and has constant material properties. The mean film thickness is h0. The layer is evaporating so that at the vapour-liquid interface there is mass loss, momentum transfer and energy consumption. The plate has a fixed constant temperature TH. Evaporative losses to the passive gas above controls the liquid temperature, TF on the free surface. The surface tension, σ_0 is a function of temperature, so that the thermo-capillary effects are present. The flow in the thin film can be represented by the Navier-Stokes, energy and continuity equations using a two-dimensional Cartesian co-ordinate system (x, z), together with no-slip condition at the solid surface, and the normal and shear stress conditions at the free surface, and the constitutive equation.

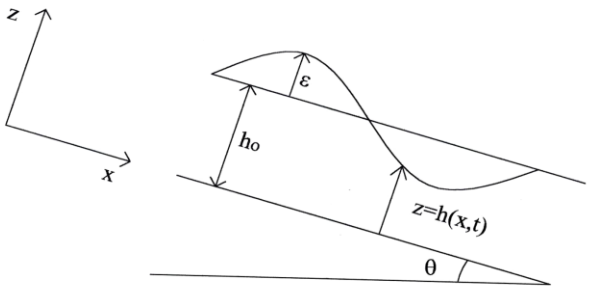

Fig. 1: The physical configuration of thin film flowing down an inclined plane. h_0 is the mean film thickness, $h(x,t)$ is the film thickness at location x and time t, ε is the initial amplitude of the disturbance wave, and θ is the inclination of the film support with the horizontal.

Following the analysis in Burelbach et al. [9] and Joo et al. [8], the governing equations for motion in thin film can be simplified under long wave approximation, to arrive at a nonlinear fourth order partial differential equation, called the 'equation of evolution' [EOE] that describes the evolution of the film interface in time t, and space x, denoted by h(x,t), and is given by [8-12].

$$h_t + \frac{E}{h+K} + Gh^2 h_x \sin\theta + \left[\frac{2}{15}G^2 h^6 h_x \sin^2\theta + \frac{KM}{P}\frac{h^2 h_x}{(h+K)^2} + \frac{E^2}{D}\frac{h^3 h_x}{(h+K)^3} - \frac{1}{3}Gh^3 h_x \cos\theta + \frac{A}{h}h_x + Sh^3 h_{xxx}\right]_x + \frac{5}{24}GE\left(\frac{h^4}{h+K}\right)_x \sin\theta + EP\left(\frac{h}{h+K}\right)^3\left[\frac{E}{3(h+K)} + \frac{G}{120}(7h-15K)hh_x \sin\theta\right] = 0 \quad (1)$$

The definitions of symbols used in Eq. 1 are given in Appendix 1. The subscripts, t and x represent the derivatives with respect to time, t and space coordinate x respectively. Eq. 1 can be solved for the film thickness h(x, t) using a space periodic initial condition,

$$h(0,x) = 1 - \varepsilon \cos kx\,;\ |\varepsilon| < 1 \quad (2)$$

with periodic boundary conditions in x-domain over a disturbance wavelength, λ=2π/k, where k is a wavenumber, and ε is the amplitude of the initial perturbation on the film surface. For a cosine wave initial condition, the boundary conditions can be expressed as [8-12],

$$\left(\frac{\partial^i h}{\partial x^i}\right)_{x=-\frac{\lambda}{2}} = \left(\frac{\partial^i h}{\partial x^i}\right)_{x=\frac{\lambda}{2}} (i = 0, 1, 2, 3);\quad -\lambda/2 \le x \le \lambda/2 \quad (3)$$

Published By:
Blue Eyes Intelligence Engineering
& Sciences Publication

2.2 Equation of evolution by Joo et al. [8]

The EOE of Joo et al. [8] is rewritten here for ease of reference and clarity of results presented later in the paper,

$$h_\tau + \frac{\bar{E}}{h+K} + Gh^2h_\xi \sin\theta + \epsilon\left[\frac{2}{15}G^2h^6h_\xi \sin^2\theta + \frac{KM}{P}\frac{h^2h_\xi}{(h+K)^2} + \frac{E^2}{D}\frac{h^3h_\xi}{(h+K)^3} - \frac{1}{3}Gh^3h_\xi cos\,\theta + Sh^3h_{\xi\xi\xi}\right]_\xi + \frac{5G}{24}\epsilon\bar{E}\left(\frac{h^4}{h+K}\right)_\xi sin\,\theta + \epsilon\bar{E}P\left(\frac{h}{h+K}\right)^3\left[\frac{\bar{E}}{3(h+K)} + \frac{G}{120}(7h-15k)hh_\xi sin\,\theta\right] = 0 \quad (4)$$

Equation (4) can be scaled back to the original non-dimensional coordinates (x, z, t) and unscaled parameters E, D, and S using following scale factor used by Joo et al. [8], and becomes identical with our EOE (Eq. 1) except that the term owing to van der Waals effect is absent in Joo et al. [8] ,

$\xi = \epsilon x, \quad \zeta = z, \quad \tau = \epsilon t$

$(E, D, S) = (\epsilon\bar{E}, \epsilon^2\bar{D}, \epsilon^{-2}\bar{S})$

Joo et al. [8] have employed the scaling factor ϵ=0.2, and $\bar{S}$= 0.1 throughout their simulations.

2.3 Numerical formulation

To fully characterize the nonlinear dynamic behaviour of flow in the heated thin film on an inclined plate, one needs to solve numerically the evolution equation (Eq. 1) for a wide range of parameter values representing different thermo-physical states. Thus we need a robust numerical method to solve Eq. 1 reliably and efficiently. Hamza et al. [10] and Hamza [11] have used implicit Crank Nicholson mid-point rule in their simulations of Eq. 1. In this paper, results from the numerical simulations using Crank-Nicholson method, an implicit finite difference (IFD) scheme are compared with those of Fourier spectral method employed by Joo et al. [8].) The implicit finite difference scheme - Crank Nicholson mid-point rule is briefly described in the following paragraph.

2.3.1 Implicit finite difference scheme - Crank-Nicholson Mid-Point Rule

The rescaled equation of evolution (Eq. 1) is discretized in its conservative form using forward difference in time and central difference in space with time averaging, resulting into a set of difference equations for the film thickness h(x,t) [10,11,13]. These equations are then solved as a set of nonlinear coupled algebraic equations by an iterative procedure of the type of Newton's method. Let subscript i denotes the space discretization and superscripts n and n+1 denote values of variables at nth and (n+1)th times. Thus, Eq. 1 after discretization and simplification appears as:

$$h_i + \frac{a_1}{h_i+K} + a_2h_i^2(h_{i+1}-h_{i-1}) + a_3\{h_{i+1}^6(h_{i+2}-h_i) - h_{i-1}^6(h_i-h_{i-2})\} + a_4\left\{\frac{h_{i+1}^2(h_{i+2}-h_i)}{(h_{i+1}+K)^2} - \frac{h_{i-1}^2(h_i-h_{i-2})}{(h_{i-1}+K)^2}\right\} + a_5\left\{\frac{h_{i+1}^3(h_{i+2}-h_i)}{(h_{i+1}+K)^3} - \frac{h_{i-1}^3(h_i-h_{i-2})}{(h_{i-1}-K)^3}\right\} + a_6\{h_{i+1}^3(h_{i+2}-h_i) - h_{i-1}^3(h_i-h_{i-2})\} + a_7\{h_{i+1}^3(-h_{i-1}+2h_i-2h_{i+2}+h_{i+3}) - h_{i-1}^3(-h_{i-3}+2h_{i-2}-2h_i+h_{i+1})\} + a_8\{h_{i+1}^{-1}(h_{i+2}-h_i) - h_{i-1}^{-1}(h_i-h_{i-2})\} + a_9\left\{\frac{h_{i+1}^4}{h_{i+1}+K} - \frac{h_{i-1}^4}{h_{i-1}+K}\right\} + a_{10}\left(\frac{h_i}{h_i+K}\right)^3\{a_{11}(h_i+K)^{-1} + a_{12}(7h_i-15K)h_i(h_{i+1}-h_{i-1})\} = C_i^n \quad (5)$$

Where the superscript, $n+1$ has been dropped from the left hand side (LHS) of Eq. 5. This equation represents a set of difference equations in h_i for i =1, 2, 3, …. The LHS gives values of h_i at the $(n+1)^{th}$ time step. C_i^n is given by the following expression evaluated at the n^{th} time step.

$$C_i^n = h_i - \left[\frac{a_1}{h_i+K} + a_2h_i^2(h_{i+1}-h_{i-1}) + a_3\{h_{i+1}^6(h_{i+1}-h_i) - h_{i-1}^6(h_i-h_{i-2})\} + a_4\left\{\frac{h_{i+1}^2(h_{i+2}-h_i)}{(h_{i+1}+K)^2} - \frac{h_{i-1}^2(h_i-h_{i-2})}{(h_{i-1}+K)^2}\right\} + a_5\left\{\frac{h_{i+1}^3(h_{i+2}-h_i)}{(h_{i+1}+K)^3} - \frac{h_{i-1}^3(h_i-h_{i-2})}{(h_{i-1}-K)^3}\right\} + a_6\{h_{i+1}^3(h_{i+2}-h_i) - h_{i-1}^3(h_i-h_{i-2})\} + a_7\{h_{i+1}^3(-h_{i-1}+2h_i-2h_{i+2}+h_{i+3}) - h_{i-1}^3(-h_{i-3}+2h_{i-2}-2h_i+h_{i+1})\} + a_8\{h_{i+1}^{-1}(h_{i+2}-h_i) - h_{i-1}^{-1}(h_i-h_{i-2})\} + a_9\left\{\frac{h_{i+1}^4}{h_{i+1}+K} - \frac{h_{i-1}^4}{h_{i-1}+K}\right\} + a_{10}\left(\frac{h_i}{h_i+K}\right)^3\{a_{11}(h_i+K)^{-1} + a_{12}(7h_i-15K)h_i(h_{i+1}-h_{i-1})\}\right] \quad (6)$$

The constants a_i (i=*1 ,2, 3, ……., 12*) are defined as:

$$a_1 = \frac{SE(\Delta\tau)}{2A^2}, a_2 = \left(\frac{S}{A}\right)^{\frac{1}{2}}\frac{Re\Delta\tau}{4\Delta xA}, a_3 = \frac{\Delta\tau}{4(\Delta x)^2}\frac{Re^2}{15A},$$

$$a_4 = \frac{\Delta\tau}{8(\Delta x)^2}\frac{KM}{PA}, a_5 = \frac{\Delta\tau}{8(\Delta x)^2}\frac{E^2}{DA},$$

$$a_6 = -\frac{\Delta\tau}{8(\Delta x)^2}\frac{G\cos\beta}{3A}, a_7 = \frac{\Delta\tau}{8(\Delta x)^4}, a_8 = \frac{\Delta\tau}{8(\Delta x)^2},$$

$$a_9 = \frac{\Delta\tau}{4\Delta x}\frac{5ERe}{24}\left(\frac{S}{A^3}\right)^{\frac{1}{2}}, a_{10} = \frac{\Delta\tau}{2}\left(\frac{S}{A^3}\right)^{\frac{1}{2}}EP,$$

$$a_{11} = \left(\frac{S}{A}\right)^{\frac{1}{2}}\frac{E}{3}, a_{12} = \frac{Re}{240\Delta x} \quad (7)$$

Eq. (5) forms a set of coupled nonlinear algebraic equations which were solved iteratively using Newton Raphson method on the MATLAB platform [14]. Twenty-one grid points in spatial domain and a time step of 0.001 was used throughout the simulations as it was found sufficient for a converged solution for the parameters investigated as evident from the mesh sensitivity analysis given in the next section. The values of physical parameters used in simulations are given in Appendix 2.

3. RESULTS AND DISCUSSION

The results of the numerical solution of the equation of evolution (EOE) given in Eq. 1 (with the van der Waals force term deleted, reduces our EOE identical to that of Joo et al. [7]) using our implicit code are compared with the numerical results from Fourier spectral method of Joo et al. [7], in figures 2 through 5. Fig. 2 depicts the gravitational instability for an isothermal layer ($\bar{E}$= E2/D = KM/P =0) for a wave number k=0.7.

Published By:
Blue Eyes Intelligence Engineering
& Sciences Publication

The free surface profiles for the time, $\tau = 0 - 2$ are almost identical to that of Joo et al. [7]. Each profile represents a time increment of 0.05, with the final profile (shown in red colour) corresponds to $\tau = 2$.

Evolution of the free surface profiles for the layer with thermo-capillarity for k=0.7 and corresponding to G=5, $\beta=30^0$, KM/P=1, K=0.1, $\bar{S}$=0.1, $\bar{E}$ = E^2/D = KM/P =0 are shown in Fig. 3 for the time range $0 \leq \tau \leq 2.9$, with a time increment of $\Delta\tau$=0.1. It may be noted that the film interface profiles are remarkably similar for the simulations based on FDM (present work) and the Spectral method (Joo et al. [7]). The profile shown in red corresponds to the last time step in each case.

Fig. 4 shows the evolution of the film interface for an evaporating layer where various nonlinear antagonistic forces lead to instability resulting into the film rupture. The interface profiles are shown for $\Delta\tau = 0.05$, and for parameter values shown in the figure caption. Our film rupture time, τ_R obtained using implicit FDM is 4.9384 that exactly conform to the rupture time τ_R=4.9388 from spectral method (Joo et al. [7]) with numerical accuracy up to 3rd decimal place.

Figures 5 shows the free surface profiles for evaporating layers with gravitational effects leading to rupture for an inclination, $\theta=15^0$. Parameters are: k=0.7, $\bar{E}$=0.1, K=0.1, P=1, $\bar{S}$=0.1, G=5, E^2/D=0.0005, KM/P=0.1, M=1, with $\Delta\tau = 0.05$. Rupture time τ_R from FD simulations is 5.1290. The rupture time τ_R from the spectral method (Joo et al. [7]) is 5.1525. The maximum deviation between values of rupture times obtained from FD method (present work) and spectral method (Joo et al. [7]) was observed to be 0.46%.

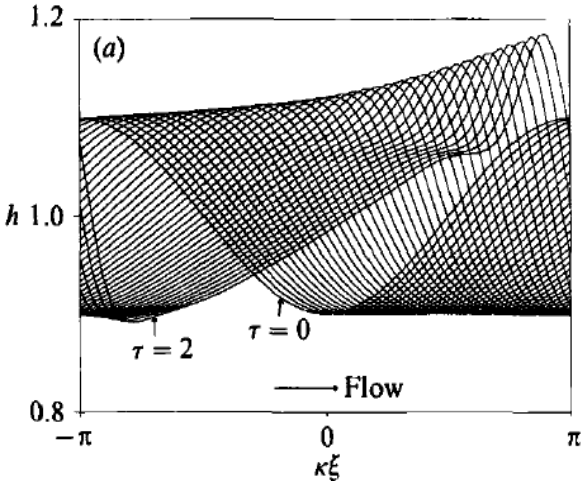

Fig. 2(i): Spectral method (Joo et al. [7], reproduced from Hamza [10])

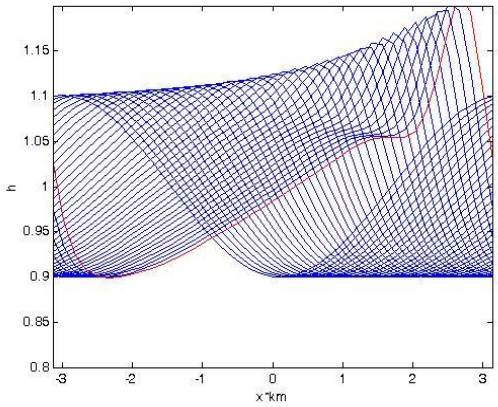

Fig. 2(ii): Implicit FDM (present work)

Fig. 2: Free surface configuration under gravitational instability for an isothermal layer with k=0.7, G=5, $\theta=45^0$ and $\bar{S}$=0.1 with $\Delta\tau$=0.05 up to τ=2. Profiles in (i) and (ii) correspond to spectral method and FDM (present work) respectively. The profile shown in red colour corresponds to $\tau = 2$.

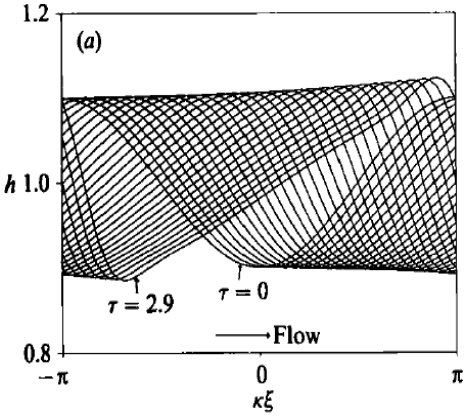

Fig. 3(i): Spectral method (Joo et al. [7], reproduced from Hamza [10])

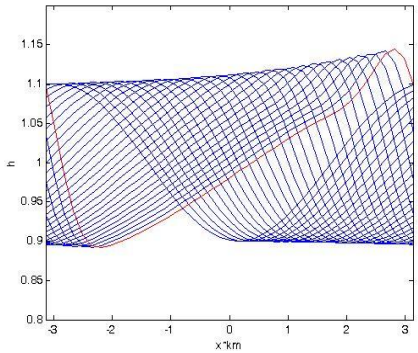

Fig. 3(ii): Implicit FDM (present work)

Fig. 3: Evolution of the free surface profile for the layer with thermocapillarity when k=0.7, G=5, β=300, KM/P=1, K=0.1, $\bar{S}$=0.1, $\bar{E}$= E2/D = KM/P =0, $0 \leq \tau \leq 2.9$ with $\Delta\tau$=0.1. Profiles in 3(i) and 3(ii) correspond to spectral method and FDM respectively. The profile shown in red colour corresponds to $\tau = 2.9$.

Published By:
Blue Eyes Intelligence Engineering
& Sciences Publication

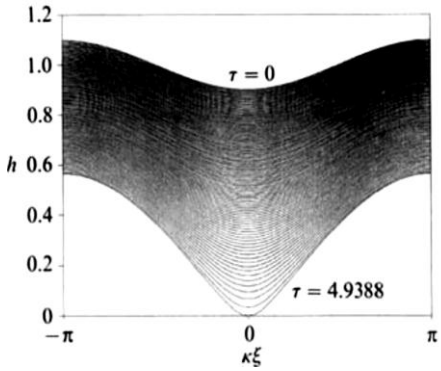

Fig. 4(i): Spectral method (Joo et al. [7], reproduced from Hamza [10])

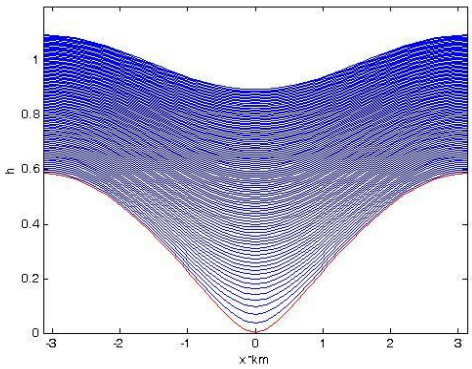

Fig. 4(ii): Implicit FDM (present work)

Fig. 4: Evolution of film instability leading to film rupture for an evaporating horizontal layer shown with Δτ = 0.05, and k = 0.7, G=0, KM/P=0, $\bar{E}$=0.1, K=0.1, P=1, and $\bar{S}$=0.1. Rupture time τ_R for spectral method (Joo et al. [7]) is 4.9388, and τ_R for implicit FDM is 4.9384 for the above parameter values. Red colour shows the surface configuration at the point of rupture.

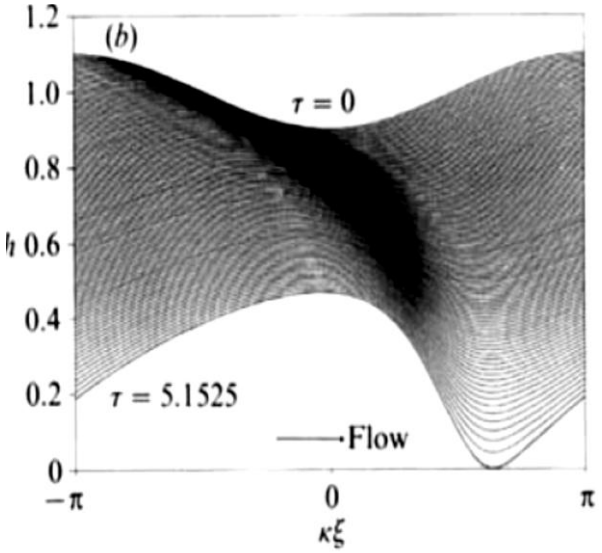

Fig. 5(i): Spectral method (Joo et al. [7], reproduced from Hamza [10])

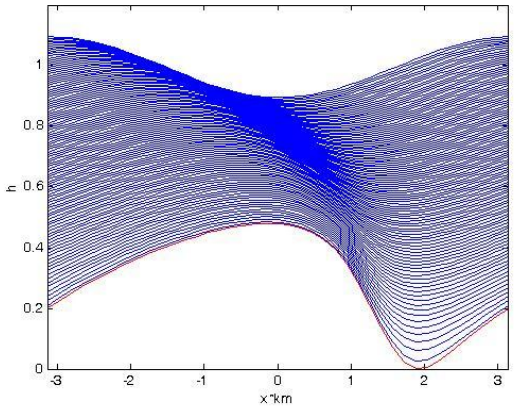

Fig. 5(ii): Implicit FDM (present work)

Fig. 5: Free surface profiles for evaporating layers with gravitational effects leading to rupture for β=150. Parameters are: k=0.7, $\bar{E}$=0.1, K=0.1, P=1, $\bar{S}$=0.1, G=5, E2/D=0.0005, KM/P=0.1, M=1, with Δτ=0.05. Rupture time from FD simulations is 5.1290. τ_R (from spectral method) = 5.1525. Deviation is 0.46%.

4.1 Mesh sensitivity analysis

The mesh sensitivity analysis for our implicit scheme was performed for the liquid layer in Fig. 4. The simulations were carried out until dry out using parameters of Fig. 4 (k = 0.7, G=0, KM/P=0, $\bar{E}$=0.1, K=0.1, P=1, and $\bar{S}$=0.1), for decreasing time steps, i.e., Δτ = 0.01, 0.05, 0.001, 0.005 and 0.0001, and increasing number of grid points, i.e., N=21, 31, 41 and 51 as shown in Table 1. It is evident from the rupture time shown in the table that the numerical solution converges (up to third decimal place) at N = 21 and Δτ = 0.001 for the film investigated.

Table 1: Rupture time for varying time step Δτ and number of grid points N for the case of Figure 6 (k = 0.7, G=0, KM/P=0.01, $\bar{E}$=0.1, K=0.1, P=1, and $\bar{S}$=0.1).

1 Δτ 2 (time step)	3 N (grid points)			
	4 21	5 31	6 41	7 51
8 0.01	9 4.9400	10 4.9400	11 4.9500	12 4.9400
13 0.05	14 4.9500	15 4.9500	16 2465.0000	17 0.4000
18 0.001	19 4.9350	20 4.9350	21 4.9350	22 4.9350
23 0.005	24 4.9350	25 4.9350	26 4.9350	27 4.9350
28 0.0001	29 4.9347	30 4.9348	31 4.9349	32 4.9349

CONCLUSIONS

We have shown comparison between an implicit finite difference scheme and Fourier spectral method applied to the problem of a thin liquid film flowing down an inclined plane subject to various physicochemical effects. These include gravity, thermo-capillarity, evaporative instabilities, surface tension and van der Waals forces. In order to solve the

Published By:
Blue Eyes Intelligence Engineering
& Sciences Publication

nonlinear evolution equation describing the dynamics, we have employed the implicit Crank Nicholson midpoint scheme and compared the results to those of Joo et al. [8] that employed Fourier spectral method. In the case where the effect of van der Waals forces are neglected, our results seem to reproduce closely the results of Joo et al. [8], with only occasional slight deviation. The cases where the instabilities lead to film rupture, the rupture time obtained using implicit FD method are in close agreement with those obtained by Joo et al. [8] within a deviation less than 1%. The cases where rupture is not reported, the film surface profiles at various times of deformation are almost identically similar in the two cases, i.e., implicit FD and spectral methods. Further, the mesh sensitivity analysis show that the numerical solutions converged for the time step 0.001 and 21 spatial grids. This implies that implicit finite difference method using Crank-Nicholson mid-point rule represents a reliable alternative method for the study of nonlinear dynamics and stability of non-isothermal thin film on inclined plane.

ACKNOWLEDGEMENT

The financial assistance from the Ministry of Higher Education of Malaysia vide grant FRGS 03-08-89 is gratefully acknowledged. The authors wish to express their gratitude to Dr. Asif Hoda (Jubail University College, Saudi Arabia) for his generous help in implementing the Fortran code on the MATLAB platform.

REFERENCES

1. Bikerman JJ (1973), Foams. Springer, New York.
2. Gaines GL (1996), Insoluble Monolayers at Liquid-gas Interfaces. Interscience, New York.
3. Sharma A & Jameel AT (1993), Nonlinear stability, rupture, and morphological phase separation of thin fluid films on apolar and polar substrates. J. Colloid and Interface Science 161,190-208.
4. Sharma A & Ruckenstein E (1986), An analytical nonlinear theory of thin film rupture and its application to wetting films. J. Colloid and Interface Science 113, 456-479.
5. Grotberg JB (1994), Pulmonary flow and transport phenomena. Annual Reviews of Fluid Mechanics 26, 529-571.
6. Wong H, Fatt I & Radke CJ (1996), Deposition and thinning of the human tear film. J. Colloid and Interface Science 184, 44-51.
7. Benny DJ (1966), Long waves on liquid films. J. Mathematics and Physics, 45, 150-155.
8. Joo SW, Davis SH & Bankoff SG (1991), Long-wave instabilities of heated falling films: two-dimensional theory of uniform layers. J. Fluid Mechanics 230, 117-146.
9. Burelbach JP, Bankoff SG & Davis SH (1988), Nonlinear stability of evaporating/condensing liquid films. J. Fluid Mechanics 195, 463–494.
10. Hamza MA, Jameel AT, Asrar W & Hoda A (2017), International Conference on Mechanical, Automotive and Aerospace Engineering 2016. IOP Conf. Series: Materials Science and Engineering 184 (2017) 012065. doi:10.1088/1757-899X/184/1/012065.
11. Hamza MA (2017), The Numerical Simulation of Non-isothermal Thin Liquid Film Flow On Inclined Plane, MS dissertation, International Islamic University Malaysia, Kuala Lumpur.
12. Ali MA, Jameel AT & Ahmadun F-R (2005), Stability and rupture of nano-liquid film (NLF) flowing down an inclined plane. Computers and Chemical Engineering 29, 2144-2154. doi: 10.1016/j.compchemeng.2005.07.003.
13. Hoffmann KA & Chiang ST (2004), Computational Fluid Dynamics: vol. 1, 4th ed. Engineering Education System, Wichita, USA.
14. Math Works Inc. (2013), MATLAB R2013a. Math Works Inc. MA, USA.

Appendix 1

Non-dimensional Parameters Occurring in the Mathematical Model

Non dimensional mean surface tension, $s = \frac{\sigma_o h_o}{3\rho v^2}$

Evaporation number, $E = \frac{k_t \Delta T}{\rho v L}$

Non dimensional Hamaker constant, $A = \frac{A'}{6\pi h_o \rho v^2}$

Non dimensional gravitational number, $G = \frac{h_o^3 g}{v^2}$

Thermal diffusivity, $\kappa = \frac{k_t}{\rho c_p}$

Marangoni number, $M = \frac{\gamma \Delta T h_o}{2\mu\kappa}$

Prandtl number, $P = \frac{c_p \mu}{k_t}$

Ratio of vapour to liquid density, $D = 10^{-3}$

Reynolds number, $Re = G \sin\theta$

Appendix 2

Nomenclature and Numerical Values of Various Parameters Used in Simulations

$\Delta\tau\ (time\ step\ in\ simulation) = 0.001$

$\rho\ (liquid\ density) = 1000\, kg/m^3$

$k_t\ (liquid\ thermal\ conductivity) = 0.613\, W/m.K$

$K\ (a\ parameter\ that\ measures\ the\ degree\ of\ non - equilibrium\ at\ the\ evaporating\ interface) = 0.1$

$c_p (liquid\ thermal\ conductivity) = 4.19\, kj/kg.K$

$L\ (latent\ heat\ of\ vaporization) = 2257 \times 10^3 J/kg$

$v\ (liquid\ kinematic\ viscosity) = 0.3548 \times 10^{-6}\, m^2/s$

$\mu_w (liquid\ viscosity) = 0.3548 \times 10^{-3}\, kg/m.s$

$\Delta T\ (= T_H - T_S) = 20K$

$\gamma\ (= \frac{d\sigma}{dt}) = 0.18 \times 10^{-3}\, N/m.℃$

$A'(Hamaker\ constant, dimensional) = 4.67 \times 10^{-20} J$

$\sigma_o (mean\ surface\ tension\ at\ the\ saturation\ temperature) = 72.8 \times 10^{-3}\, J/m^2$

$\varepsilon\ (amplitude\ of\ initial\ disturbance\ on\ the\ film\ surface) = 0.1$

Published By:
Blue Eyes Intelligence Engineering
& Sciences Publication